Macromolecules
Volume 24, Number 1 January 7, 1991

Electroactive Ladder Polyquinoxalines. 1. Properties of the Model Compound 5,12-Dihydro-5,7,12,14-tetraazapentacene and Its Complexes

Samson A. Jenekhe

Department of Chemical Engineering, University of Rochester, Rochester, New York 14627

Received July 25, 1989; Revised Manuscript Received May 21, 1990

ABSTRACT: Studies of the structural and physicochemical properties of a model compound of ladder polyquinoxalines, 5,12-dihydro-5,7,12,14-tetraazapentacene (DHTAP), including X-ray diffraction, morphology, spectroscopy, electrochemistry, complex formation, and electrical conductivity are reported. DHTAP has a melting point of 545 °C, which is close to its decomposition temperature, and insulating electrical properties. Its solution- and solid-state electronic absorption spectra have two characteristic intense bands, near 300 and 600 nm, due to π–π^* transitions. DHTAP and its complexes exhibit strong fluorescence in solution; the observed dependence of the emission properties on concentration and solvent is attributed to aggregation phenomena in solution at high concentrations. It is shown that a conductive crystalline DHTAP salt complex formed by reaction with methanesulfonic acid (MSA) has the structure of a methanesulfonate salt of the 7,14-protonated DHTAP. The highly anisotropic crystals of the DHTAP/MSA complex are soluble in common polar organic solvents, melt at 138 °C, and have a pressed dc conductivity of about 10^{-2} S/cm at room temperature. It is suggested that these results on DHTAP and its complexes have direct implications for the high molecular weight ladder polyquinoxalines.

Introduction

Numerous *ladder* or *double-stranded* polymers have been synthesized and widely studied[1-17] since the early 1960s, including major synthetic and thermal stability characterization efforts on aromatic and heterocyclic types of ladder polymers at the Air Force Materials Laboratory[1-6] and in Stille's[7-10] and Marvel's[13-15] research groups. However, the solid-state properties of this class of polymers, especially electronic and optical properties, have largely been neglected until very recently.[17-20]

Our current interest in the electronic, linear and nonlinear optical, and electrochemical properties of conjugated ladder polymers,[19,20] stems in part from their greater structural order compared to most single-stranded conjugated polymers and their generally excellent thermal stability, mechanical strength, and resistance to degradation. The rigid-rod nature of the backbone of conjugated ladder polymers suggests that anisotropy would be a central feature of their morphology and physical properties.[20c] In this regard, it should be noted that π-conjugated ladder polymers provide a structural bridge between the single-stranded quasi one-dimensional conjugated polymers and two-dimensional graphite. Ladder polyquinoxalines have additional attractive features: (i) variations of ladder polyquinoxalines and related ladder polymers containing a 1,4-pyrazine ring can be synthesized by using a number of synthetic routes;[7-13,16] (ii) the highly regular or symmetric chain structure and composition and planar chain conformation of the ladder polyquinoxalines can be expected to favor crystallization, not previously reported in ladder polymers; and (iii) although the band structure and electronic properties of the ladder polyquinoxalines have not yet been calculated, their molecular structures are intermediate between polyacene and paracyanogen (i.e., a 1,4-pyrazine-type ladder), which are predicted to be intrinsic semiconductors with small band-gaps or metals with a zero band-gap.[21-26]

The structural and physicochemical properties of the model compound 5,12-dihydro-5,7,12,14-tetraazapentacene (II or DHTAP) have direct implications for the higher

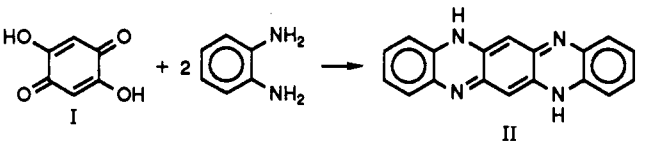

I II

molecular weight ladder polyquinoxalines. Also, the properties of DHTAP are of interest per se; it is desirable to compare the structural and physical properties to the parent fused hydrocarbon, pentacene, whose crystal structure,[27] electronic, and optical properties have been widely studied.[27-29] Although previously synthesized[9,30] and its molecular structure established via synthetic methods by Badger and Pettit,[30] very little is known about

0024-9297/91/2224-0001$02.50/0

Table I
Solubility and Appearance of Solutions of DHTAP and DHTAP/MAS Crystals

solvent	ϵ'	DHTAP powder		DHTAP/MAS crystals	
		solubility[a]	appearance	solubility[a]	appearance
glacial acetic acid	6.15	NS		VS	blue soln; red fluorescence
aniline	6.89	SS	red soln; residual solid	SS	reddish/purple soln; residual crystals
N,N-dimethylacetamine (DMAc)		SS	lt red soln; resid solid	VS	blue soln
N,N-dimethylformamide (DMF)	36.7	SS	opaque red soln; residual solid	VS	blue soln; red fluorescence
dimethyl sulfoxide (DMSO)	49	SS	red soln; residual solid	VS	blue soln
acetonitrile	36.2			SS	lt blue soln; crystals remain
acetone	21.2			SS	pink soln; crystals remain
N-methyl-2-pyrrolidone (NMP)		SS	opaque red soln; residual solid	VS	blue soln; red fluorescence
methanol	32.63	NS		VS	blue soln; red fluorescence
methyl ethyl ketone (MEK)		NS		NS	
methylene chloride	9.08	NS		NS	
pyridine	12.3	SS	red soln	S	red soln; residual crystals
tetrahydrofuran (THF)	7.6	NS		SS	pink soln; crystals remain
toluene	2.38	NS		NS	
nitromethane	36	NS		SS	lt blue soln; crystals remain
nitrobenzene	34.82	SS	lt grn soln	NS	
methanesulfonic acid (MSA)		VS	blue soln; red fluorescence	VS	blue soln; red fluorescence
concd H_2SO_4		VS	blue soln; red fluorescence	VS	blue soln; red fluorescence
water	78	NS		SS	blue soln

[a] NS = not soluble. S = soluble. SS = slightly soluble. VS = very soluble.

its properties: for example, even the melting point has not been reported. We have prepared DHTAP according to the scheme suggested by Stille and co-workers[9,10] and carried out the condensation in polyphosphoric acid (PPA) under conditions similar to the synthesis of the corresponding high molecular weight polymer.

Our studies of DHTAP reported here include crystallization and melting, X-ray diffraction, morphology, spectroscopy, electrochemistry, complex formation, and electrical conductivity. We have discovered that DHTAP forms conductive crystalline complexes, and one of these, a 7,14-protonated DHTAP methanesulfonate salt, is also studied in detail. Our studies of the third-order nonlinear optical properties of DHTAP and its complexes as solutions and thin films found a surprisingly large picosecond degenerate four-wave mixing[19b] $\chi_{xxxx}^{(3)}(\omega)$ and a large picosecond third harmonic[19c] $\chi^{(3)}(-3\omega;\omega,\omega,\omega)$ as will be reported elsewhere.[19b,c]

Experimental Section

Synthesis and Purification of DHTAP. A reaction mixture of 13.007 g (71.84 mmol) of *o*-phenylenediamine dihydrochloride and 5.032 g (35.92 mmol) of 2,5-dihydroxy-*p*-benzoquinone in 55.282 g of 77% poly(phosphoric acid) (PPA) was prepared in a flask. The reaction mixture was heated in nitrogen atmosphere: first, to 110 °C overnight (15 h) and finally to 170–175 °C for 19 h. The metallic green solution was cooled and poured into 1000 mL of methanol. A deep blue-purple powder was recovered. DSC revealed low-melting impurities (<200 °C) in this product. The product was refluxed in 2000 mL of water twice for a total of 24 h, washed with acetone, and dried in vacuo at room temperature (25 °C). The resulting deep blue-purple product had a sharp melting point of 545 °C as determined by DSC (heating rate 7.5 °C/min). FTIR spectrum: 3440 (vs), 2928 (w), 1630 (vs), 1530 (vs), 1472 (s), 1245 (vs), 1152 (s), 1030 (s), 904 (w), 820 (s), 758 (s), 600 (w), 535 (w), 500 (w) cm^{-1}.

Thin films of the pure unprotonated DHTAP on glass and other substrates were generally prepared by evaporation of a dilute solution (≤0.05 M) in either MSA or concentrated sulfuric acid followed by repeated soaking in water. Such films were purple-gold in reflection and purple-red in transmission. These DHTAP thin films were free of acids or protonation as evidenced by their insulating properties and insolubility when immersed in organic solvents such as methanol, acetic acid, DMF, DMAc, or DMSO. Films of the protonated salt complexes of DHTAP, whose preparation is described below, in contrast to the unprotonated DHTAP, were conductive and dissolve to give blue solutions when immersed in organic solvents (e.g., DMF, methanol, acetic acid, DMSO, etc.).

DHTAP Salt Complexes. DHTAP samples can be recrystallized from its acid solutions; for example, when a solution of DHTAP in methanesulfonic acid (MSA) was poured into a large volume of acetone, a crystalline greenish to blue-purple powder was precipitated and recovered. However, when a concentrated solution of DHTAP in MSA was placed on a glass slide or a shallow Petri dish, gold-yellow needlelike crystals began to grow in about 1 day, reaching macroscopic sizes (~1 mm to 1 cm in length) after several days. Preliminary measurements showed that these needlelike crystals were highly conductive, unlike authentic blue-purple DHTAP, and also they showed a different melting point compared to the parent compound. These initial observations suggested the formation of a complex between DHTAP and MSA. Samples of such a DHTAP/MSA complex were subsequently produced for a detailed study as follows: (a) 10–15 mL of a 0.24 M DHTAP solution in MSA was placed in a 14.5-cm-diameter Petri dish or a very shallow large (19 cm in diameter) beaker and allowed to crystallize at room temperature (23 °C) for at least 4 days. The brilliant gold-yellow crystals were recovered by adding 20–50 mL of acetone followed by vacuum filtration through No. 44 Whatman filter paper and a Buchner funnel; the recovered crystals were thoroughly washed with 150–200 mL of acetone and vacuum dried at 25 or 100 °C for 2 h. The yield was about 86%. Elem anal. Calcd for $(C_{18}H_{12}N_4)(CH_3SO_3H)_2$: C, 50.41; H, 4.23; N, 11.76; S, 13.46; O, 20.15. Found: C, 48.78; H, 4.26; N, 10.86; S, 12.77; O, 23.51. (b) Conductive gold-yellow crystals of the DHTAP/MSA complex were also prepared by solvent evaporation from liquid films of concentrated DHTAP/MSA solutions (0.3 M) on various substrates (glass, silicon wafers) heated on a hot plate. Conductive polycrystalline films exhibiting different morphologies were obtained by this technique. Films cast from dilute MSA solutions (≤0.05 M) and washed in water were insulators and not conductive.

Solubility. The qualitative solubility of DHTAP powder and DHTAP/MSA crystals in various solvents was determined by placing ~2 mg of sample in a test tube and adding the solvent (~5 mL). In cases where ready solubilization did not occur, the solubility test results were recorded after 1–5 weeks. Table I shows the solubility and appearance of solutions.

Characterization. A. Differential Scanning Calorimetry (DSC). Thermal analysis, including DSC and thermogravimetric analysis (TGA), was done by using a Du Pont Model 1090B thermal analyzer equipped with a DSC cell module and a Model 991 TGA module. An indium (156.6 °C) and zinc (419.4 °C) DSC standards were used to calibrate the accuracy of measured transition (melting) points. Samples were sealed in DSC pans and run from 25 to 600 °C at 7.5 °C/min. TGA runs were

performed in air or nitrogen atmospheres at a heating rate of 7.5 °C/min.

B. Infrared Spectra. Fourier transform infrared (FTIR) spectra of thin films cast on sapphire or KCl plates or KBr mulls were obtained by using a Digilab Model FTS-14 spectrometer. Thin films of DHTAP were cast from a very dilute (<0.05 M) MSA or sulfuric acid solution. Thin films of the DHTAP/MSA complex were cast from a methanol, *N,N*-dimethylformamide (DMF), or dimethyl sulfoxide (DMSO) solution.

C. UV-visible-near infrared spectra of DHTAP were obtained in concentrated sulfuric acid and methanesulfonic acid solutions by using a Perkin-Elmer Model Lambda 9 UV-vis-near-IR spectrophotometer in the wavelength range 185–3200 nm. Solutions with concentrations in the 10^{-4}–10^{-2} mol/L range were studied in 1-mm cells. Thin films of DHTAP (from a very dilute solution, <0.05 M) and the DHTAP/MSA complex were cast from MSA and DMSO solutions, respectively, on sapphire substrates. Solution spectra of DHTAP/MSA in methanol and pyridine were obtained by using 10^{-4} M solutions.

D. Fluorescence Emission Spectra. The fluorescence emission spectra of DHTAP and its complex, DHTAP/MSA, were obtained in solutions of varying concentration at room temperature (23 °C) by using a Perkin-Elmer Model MPF-2A fluorescence spectrometer, 5-mm cells, and a number of excitation wavelengths. The emission spectra of DHTAP in concentrated sulfuric acid solutions were obtained at several concentrations from $\sim 10^{-6}$ to $\sim 10^{-3}$ M. The emission spectra of the DHTAP/MSA complex in concentrated H_2SO_4, DMF, and MeOH solutions were also obtained at several concentrations.

E. X-ray diffraction patterns of samples were obtained by using a Rigaku powder X-ray diffractometer and computerized diffraction analyzer with a sealed-tube Cu Kα X-ray radiation at 1.540 562-Å wavelength. The 2θ scans were from 3 to 93°, with step size of 0.02° and a 1-s counting/step. Powered samples of crystallites were held on a single-crystal silicon wafer with grease. The silicon wafer was detuned 2° to suppress reflections from the Si crystal.

F. SEM and Optical Microscopy. The morphology of as-synthesized and vacuum-baked (30 °C) crystals of the DHTAP/MSA complex was observed with an optical microscope and a JEOL Model JSM 810AII scanning electron microscope (SEM).

G. Electrical Conductivity. The dc conductivity measurements were made on compressed pellets of DHTAP and the DHTAP/MSA complex and on films of the complex cast on glass slides using two-point and four-point probe techniques. Electrical contacts were made by using a conductive silver paste. The differences between the two techniques were within experimental errors.

H. Electrochemical Experiments and Cyclic Voltammetry. All electrochemical experiments were performed in a three-electrode, single-compartment cell of about 50-mL volume using a double-junction Ag/Ag^+ ($AgNO_3$) reference electrode. Cyclic voltammograms of polycrystalline films of DHTAP on a platinum electrode, prepared by solvent evaporation of dilute MSA solution (<0.1 M) on a hot plate and repeated soaking in water, were obtained by using a platinum flag as the working electrode and a platinum spiral as the counter electrode in 0.1 M tetraethylammonium perchlorate (TEAP)/acetonitrile. Cyclic voltammograms of the DHTAP/MSA complex in solution were obtained by using 10^{-3} M solutions in 0.1 M TEAP/DMSO and a platinum wire and a platinum spiral as working and counter electrodes, respectively. Attempts were made to obtain solution cyclic voltammograms of pristine DHTAP in aqueous H_2SO_4 solutions (10^{-4} and 10^{-2} M), but there were too many redox couples that could not be reproduced. All the electrochemical experiments were performed by using a programmable EG&G Princeton Applied Research Model 273 potentiostat/galvanostat and Model RE0091 X-Y recorder.

Results and Discussion

Structure, Complexes, and Morphology. The structure of DHTAP has previously been established[9,30] as well as the present synthetic scheme.[30] The IR spectrum of the pristine DHTAP sample was consistent with the structure II. In particular, the bands at 3440, 1630, and 1245 cm^{-1} are assigned to ν(N–H), ν(C=N), and ν(C–N), respectively.

Elemental analysis of DHTAP/MSA crystals showed elemental composition corresponding to $(C_{18}H_{12}N_4)(CH_3SO_3H)_2$. The structure of the DHTAP/MSA complex suggested from the infrared spectrum and elemental analysis is the salt

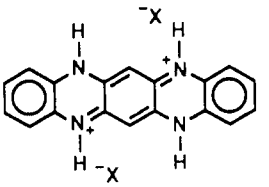

where X^- is the methanesulfonate anion. This structure is also consistent with the high conductivity of the complex and its ready solubility in polar solvents. It is expected that similar 1:2 salts of protonated DHTAP, i.e., $(DHTAPH_2)^{2+}(X^-)_2$, can be prepared from other anions (X^-). In preliminary experiments under similar crystal-growth conditions, a conductive bisulfate anion salt of $DHTAPH_2^{2+}$ crystallized from concentrated sulfuric acid solutions after several weeks; films slowly cast from the concentrated H_2SO_4 solutions (0.3 M) were also conductive. However, salts of $X^- = Cl^-$ did not crystallize from concentrated hydrochloric acid solutions in part because of the poor solubility of DHTAP in the acid. Besides the present simple salts of the 7,14-protonated DHTAP, i.e., $(DHTAPH_2)^{2+}(X^-)_2$, crystalline complexes of the unprotonated DHTAP with acceptors like TCNQ[31-33] can be expected to form and to be more conductive in view of precedents like phenazine/TCNQ complexes, which are metals with single-crystal room-temperature conductivities as high as 100 S/cm.[34]

Figure 1A shows the X-ray diffraction (XRD) pattern of powdered samples of DHTAP. Although the XRD pattern indicates a highly crystalline sample, there is also the presence of amorphous components. The *d*-spacings at 9.81, 4.96, and 3.27 Å, which are also the most intense, correspond to (001), (002), and (0003) reflections, respectively. Thus, one of the unit cell parameters is ~9.81 Å. However, all the *d*-spacings of Figure 1A are yet to be indexed; so, the unit cell and crystallographic structure of DHTAP remain unknown. The parent pentacene has a triclinic unit cell with a *c* parameter of 16.01 Å.[27,28] An XRD pattern taken from a DHTAP compressed pellet (3600 psi) was found to be virtually identical with Figure 1A, except that an additional peak appeared at 13.56 Å and the 9.81-Å peak became the most intense. This suggests that more reflection peaks will be found with a much purer and more crystalline sample of DHTAP.

The XRD pattern of the gold-yellow crystals of the DHTAP/MSA complex is shown in Figure 1B. This pattern, when compared to that of DHTAP in Figure 1A, indicates that the methanesulfonate salt of protonated DHTAP has a completely different crystal structure. Also, the very sharp XRD peaks in Figure 1B and their relatively large intensities compared to Figure 1A indicate that the complex is fully crystalline with no amorphous regions or impurities. The XRD pattern of the DHTAP/MSA complex also suggests that the relatively broad and low intensity peaks of the pristine DHTAP powder may be due to amorphous impurities. Attempts to identify the crystal symmetry by a fit to the observed 30 reflections in the powder data of Figure 1B were unsuccessful. However, the crystal structure was narrowed to either a monoclinic or triclinic symmetry. Weissenberg photographs gave

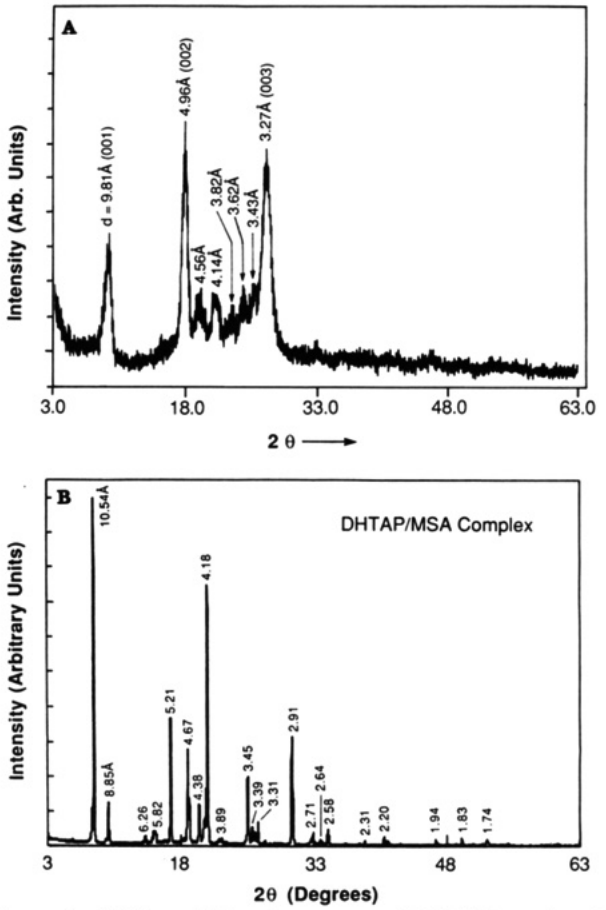

Figure 1. (A) X-ray diffraction pattern of DHTAP powder. (B) X-ray diffraction pattern of the DHTAP/MSA complex.

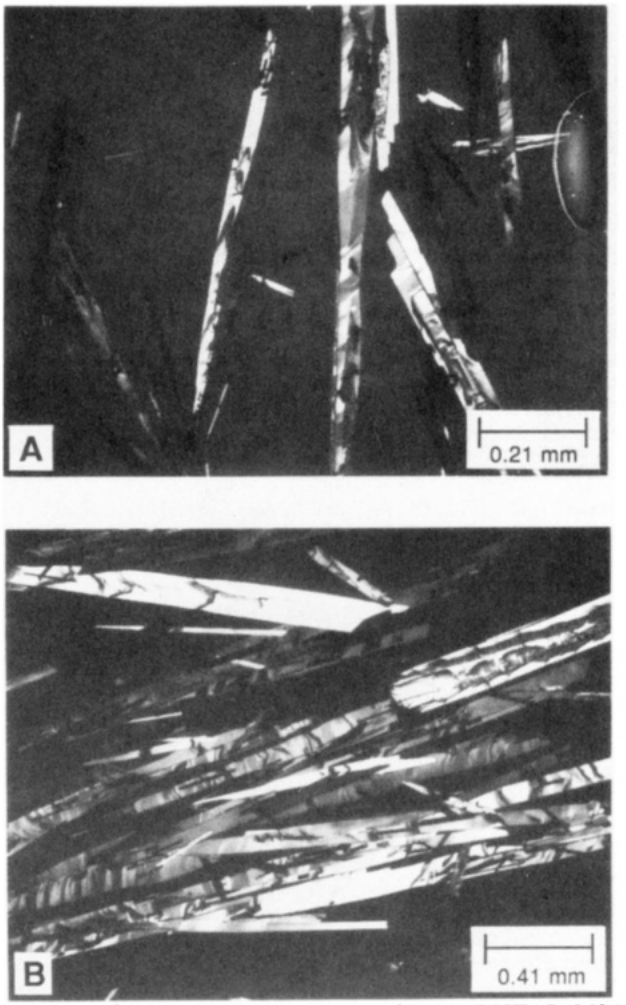

Figure 2. Optical micrographs of conductive DHTAP/MSA crystals.

one of the unit cell parameters to be ~21.54 Å. Measured characteristic cleavage angles were 109° and 116°. Determination of the true crystallographic structure of DHTAP and its complexes will require growth of large single crystals.

The macroscopic crystals of the conductive DHTAP/MSA complex, as-synthesized from a concentrated MSA solution of DHTAP, are highly anisotropic, as shown in the optical micrographs of Figures 2 and 3. Though the gold-yellow crystals are needlelike in overall appearance, the needles are aggregates of rectangular platelets, as revealed in the optical micrographs and in SEM pictures (Figure 4) of vacuum-baked DHTAP/MSA crystals grown from a concentrated MSA solution of DHTAP on a silicon wafer at room temperature. Steps along the needle axis are evident in the crystals. The layered nature of the crystals is revealed by the steps and cleavage planes. The large needlelike crystals had lengths of up to 20–80 mm and diameters up to 0.1–0.4 mm. However, some of the constituent platelets were as small as 10 μm wide by 30–60 μm in length and as thin as 0.4–1.0 μm. In contrast to the crystal morphologies shown in Figures 2–4, crystals of the DHTAP/MSA complex grown on glass or silicon wafer substrates by evaporation of a concentrated (0.25 M) MSA solution on a hot plate generally exhibited a spherulitic morphology with a fibrous substructure in the radial direction.

Thermal Properties. Figure 5 shows the thermal stability of DHTAP and its methanesulfonate complex in nitrogen atmosphere as determined by TGA. A slight weight loss of about 1–3% in DHTAP between 300 and 530 °C is followed by a very slow weight loss between about 550 and 800 °C where a residue of about 70% is obtained. The few percent weight loss at ~300 °C is probably due to partial sublimation evidenced by a thin blue coating on the TGA quartz tube wall. It is known that DHTAP sublimes at 280–290 °C under moderate vacuum (0.1 Torr).[9,30] Crystals of the DHTAP/MSA complex are less stable than the parent compound; onset of significant thermal decomposition is observed at ~300 °C. After the initial major weight loss of 55% up to 500 °C, very slow weight loss continues and results in about 38% residue at 750 °C.

The DSC thermograms of DHTAP and the DHTAP/MSA complex are shown in Figures 6 and 7, respectively. The sharp endothermic peak in Figure 6 is interpreted as the melting of DHTAP in light of the above TGA data, which show its relative stability up to such a high temperature. The peak melting point of DHTAP determined from Figure 6 is 545 °C; an estimated heat of fusion obtained by integration of the endothermic peak and the total mass (crystalline and amorphous) is 45.5 kJ/mol (10.9 kcal/mol). This high melting point is what might be expected from its molecular structure. Also, it was previously reported that the melting point of DHTAP could not be determined in sealed tubes, apparently up to 400–450 °C.[9,30] It is to be noted that the melting point of DHTAP is very close to its decomposition temperature as the TGA data already indicated. Repeated DSC scans of several DHTAP samples also showed partial decomposition prior to the melting point (545 °C). However, the sharp melting point was always observed. The peak melting point of the DHTAP/MSA complex is 138 °C

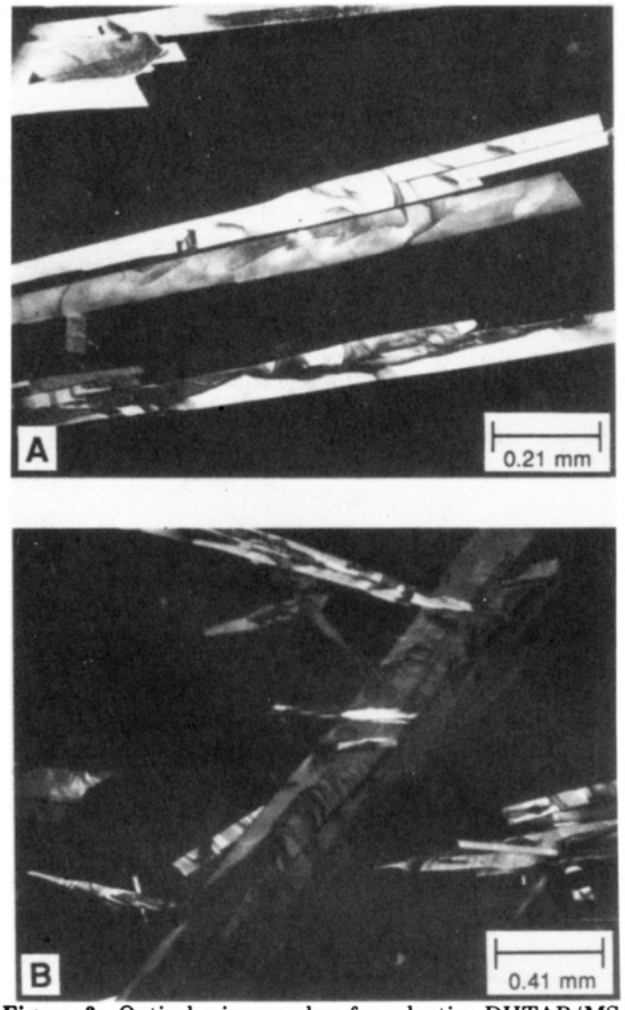

Figure 3. Optical micrographs of conductive DHTAP/MSA crystals.

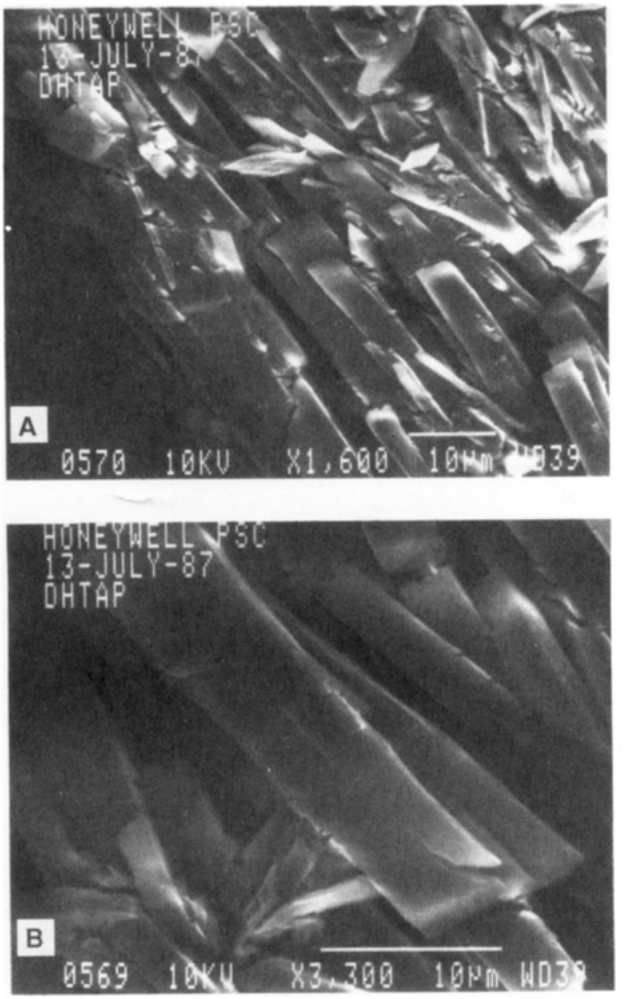

Figure 4. SEM micrograph of DHTAP/MSA crystallites.

(Figure 7), and the estimated heat of fusion is 84.6 kJ/mol (20.2 kcal/mol).

Electronic Absorption and Emission Spectra. The electronic absorption spectrum of DHTAP in methanesulfonic acid solution is shown in Figure 8 (curve 1). The optical absorption maximum (λ_{max}) is 622 nm (1.97 eV), with a corresponding ϵ value of 10^5 L mol^{-1} cm^{-1}. The other absorption bands and molar absorptivities are as follows: λ (ϵ) 571 nm (33 000); 527 nm (8800); 293 nm (51 000); 272 nm (45 000). A virtually identical electronic absorption spectrum was obtained in sulfuric acid solution: 628 nm ($\epsilon = 1.13 \times 10^5$), 576 nm (37 000), 535 nm (10 300), 294 nm (53 000), 271 nm (45 000). A characteristic feature of the solution electronic spectra of DHTAP is the two relatively narrow and intense absorption bands, one near 300 nm and the other near 600 nm. Although there are no molecular orbital calculations or models of the electronic structure and optical properties of DHTAP or closely related molecules that could be used to fully understand the nature of the observed electronic transitions, the two distinct absorption bands are attributable to π–π^* excitations. Figure 8 (curve 2) shows the electronic absorption spectrum of DHTAP thin film. The characteristic two absorption bands near 300 and 600 nm observed in solution are preserved in the thin-film spectrum. However, in the solid-state spectrum, these two bands are broadened and the absorption maximum (λ_{max}) of the "600-nm band" is red shifted to 648 nm (1.91 eV) and 593 nm respectively from 622 and 571 nm in solution. The observed high degree of π-electron delocalization in DHTAP or its protonated form

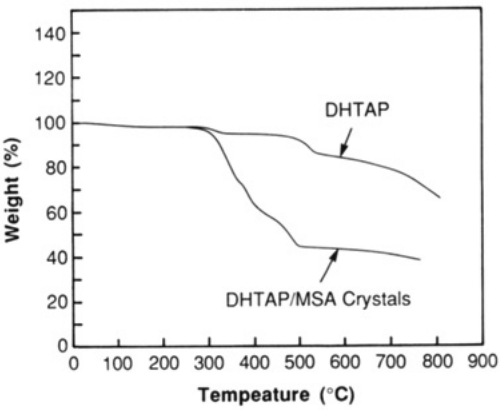

Figure 5. Thermal stability of DHTAP and the DHTAP/MSA complex in nitrogen atmosphere; 7.5 °C/min heating rate.

in solution is what might be expected for the essentially substituted planar tetraazapentacene. This is to be compared to a band-gap of 2.20 ± 0.3 eV reported for pentacene.[28]

Figure 9 shows the solution electronic absorption spectra of the DHTAP/MSA complex in methanol and pyridine. Clearly, the spectra have the same structure as those of the pure DHTAP, as one would expect since essentially the same chromophore is present in both. However, we see differences between these solution spectra of the DHTAP/MSA complex from both the corresponding solution- and solid-state spectra of the pure DHTAP. First, the absorption maximum of the "300-nm band" in the DHTAP/MSA complex at 284 nm ($\epsilon = 3.87 \times 10^5$) has no

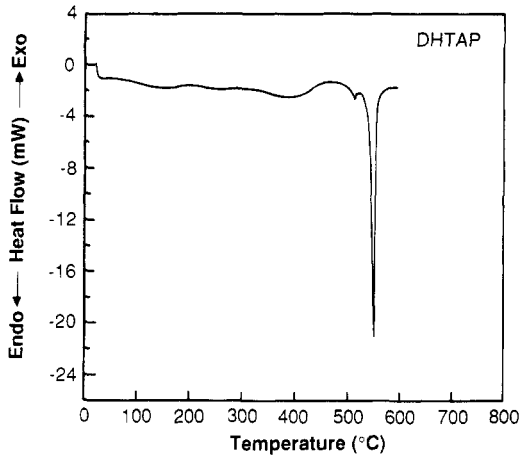

Figure 6. DSC thermogram of DHTAP obtained at a heating rate of 7.5 °C/min.

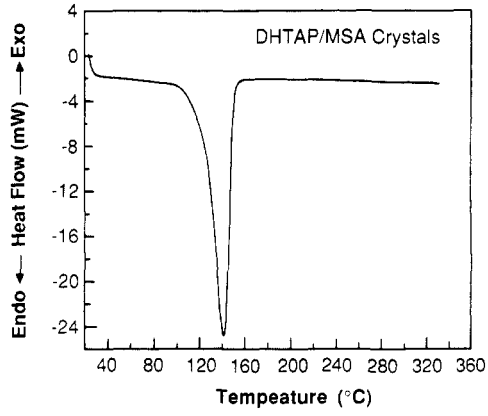

Figure 7. DSC thermogram of the DHTAP/MSA complex obtained at a heating rate of 7.5 °C/min.

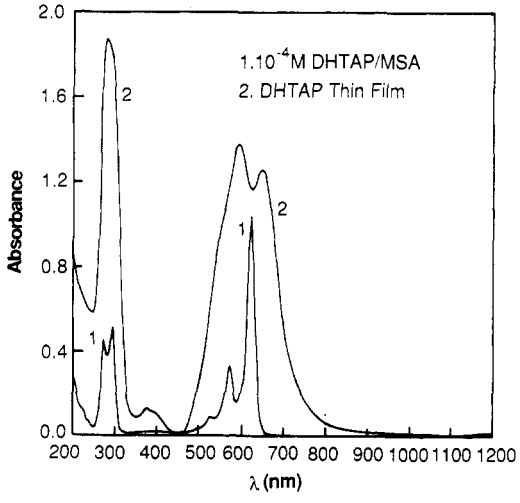

Figure 8. Electronic absorption spectra of (1) a 10^{-4} M solution of DHTAP in MSA and (2) unprotonated DHTAP thin film cast from a dilute MSA solution.

splitting and is more intense and broader, compared to DHTAP in protonic acid solution. Second, although the "600-nm band" of pure DHTAP in Figure 8 is at the same position as the methanol solution of the complex (λ_{max} = 626 and 576 nm), it is considerably broader. The complex in pyridine exhibits a broader "600-nm band", which is blue shifted to λ_{max} = 549 nm ($\epsilon = 2.0 \times 10^4$) and 516 nm ($\epsilon = 2.1 \times 10^4$). Unfortunately, because of the absorption of pyridine below 300 nm, the "300-nm band" of the complex in pyridine could not be observed. Third, the observed blue shift of the DHTAP/MSA spectrum in pyridine

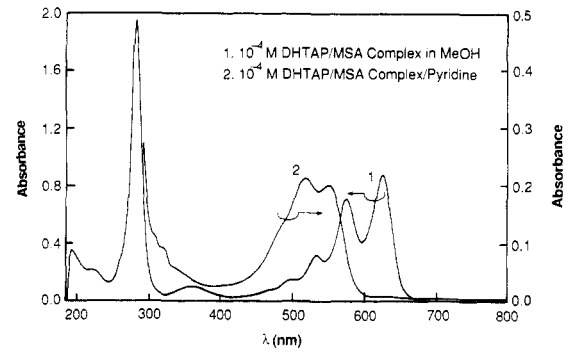

Figure 9. Electronic absorption spectra of the DHTAP/MSA complex in solution: (1) 10^{-4} M methanol solution and (2) 10^{-4} M pyridine solution.

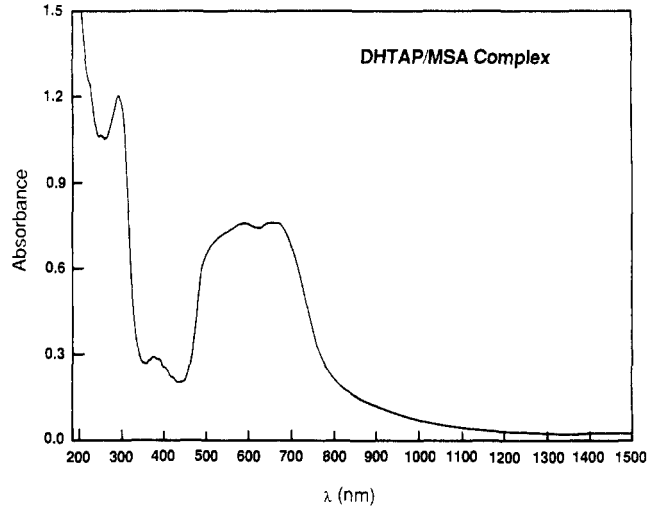

Figure 10. Electronic absorption spectrum of a thin film of the DHTAP/MSA complex cast from a methanol solution.

relative to methanol is attributed to the deprotonation of the complex to the pure unprotonated DHTAP. This was confirmed by the similarity of the red solution of the DHTAP/MSA complex in pyridine to the red solution of the powdered unprotonated DHTAP in pyridine (Table I). Thus, the protonated form of DHTAP in solution or solid state has a higher degree of π-electron delocalization than the unprotonated form.

The absorption spectrum of a thin film of the DHTAP/MSA complex in the solid state is shown in Figure 10. The characteristic two absorption bands observed near 300 and 600 nm in solution are also observed; the "300-nm band" is located at 294 nm. However, the "600-nm band" actually consists of two peaks at 663 and 590 nm merged into a very broad single band (450–800 nm) with the center at 616 nm. Comparison of all the absorption spectra of DHTAP and the DHTAP/MSA complex in in solution and solid state (Figures 8–10) shows that broadening of the absorption bands is the primary effect of increasing the solution concentration ultimately to the solid state. This is to be contrasted with emission properties, which depend strongly on concentration and solvent.

The red fluorescence of concentrated sulfuric acid solutions of DHTAP was already visually observed and mentioned by Badger and Pettit.[30] The deep blue acid (H_2SO_4, MSA) solutions of DHTAP exhibit visually observable red fluorescence as well as films cast on substrates from these solutions. Transparent blue films of DHTAP/polystyrene blends cast from concentrated H_2SO_4 also show red fluorescence. The typical fluorescence emission spectra of solutions of DHTAP or its methanesulfonate complex (DHTAP/MSA) are shown in Figures

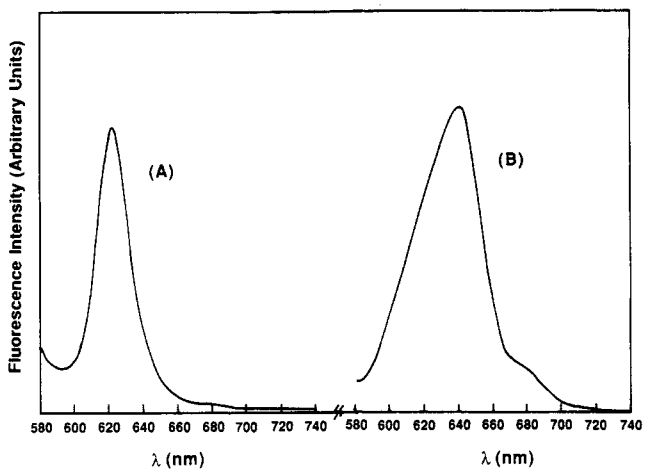

Figure 11. Fluorescence emission spectra of DHTAP solutions in concentrated H_2SO_4, excited at 566 nm: (A) 1.9×10^{-6} M; (B) 1.9×10^{-4} M.

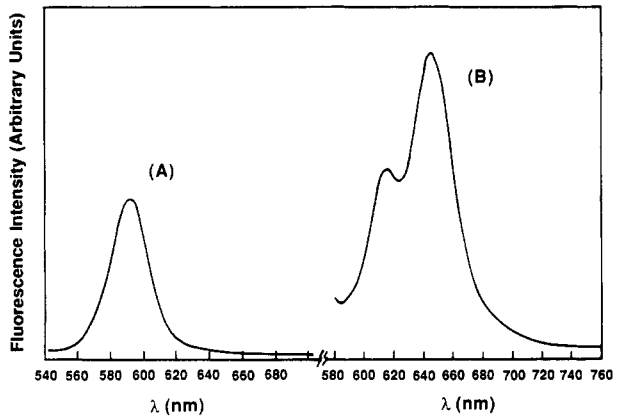

Figure 12. Fluorescence emission spectra of the DHTAP/MSA complex solutions in MeOH, excited at 566 nm: (A) 1.2×10^{-5} M; (B) 1.38×10^{-4} M.

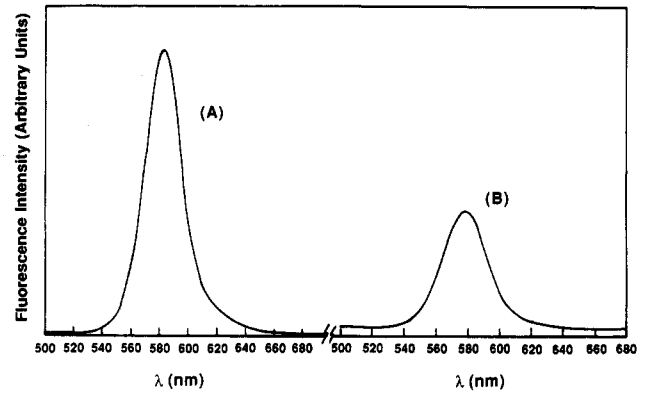

Figure 13. Fluorescence emission spectra of the DHTAP/MSA complex solutions in DMF, excited at 470 nm: (A) 1.36×10^{-6} M; (B) 1.65×10^{-4} M.

11–13. Emission from concentrated H_2SO_4 solutions of the pristine DHTAP excited at 566 nm is shown in Figure 11. Emission spectra of the DHTAP/MSA complex in methanol and DMF solutions are shown in Figures 12 and 13, respectively. One characteristic feature of the emission spectra is that a more symmetric and relatively sharp spectrum is generally obtained at very low concentrations than at high concentrations. In the case of the DHTAP/MSA solution in MeOH, two fluorescence peaks are observed at the high concentration (1.38×10^{-4} M) compared with one peak at the low concentration (1.2×10^{-5} M). The observed fluorescence emission maximum (λ_{max}^e) in solutions of DHTAP and its complex are shown

Table II
Fluorescence Emission Properties of DHTAP and Its Complexes in Solution in Different Solvents at 566-nm Excitation Wavelength

DHTAP in H_2SO_4		DHTAP/MSA in MeOH		DHTAP/MSA in DMF	
concn, M	λ_{max}^e, nm	concn, M	λ_{max}^e, nm	concn, M	λ_{max}^e, nm
1.9×10^{-6}	622	1.2×10^{-5}	591	1.36×10^{-6}	580[b]
3.3×10^{-6}	622	1.2×10^{-5}	592[a]	1.45×10^{-5}	578[b]
8.6×10^{-6}	622	1.38×10^{-4}	645 (615)	1.65×10^{-4}	582[b]
1.6×10^{-5}	622				
2.5×10^{-5}	626				
3.5×10^{-5}	635				
4.0×10^{-5}	637.5				
6.0×10^{-5}	640				
8.0×10^{-5}	641 (615)				
9.5×10^{-5}	640				
1.9×10^{-4}	640				

[a] Excitation wavelength at 530 nm. [b] Excitation wavelength at 470 nm.

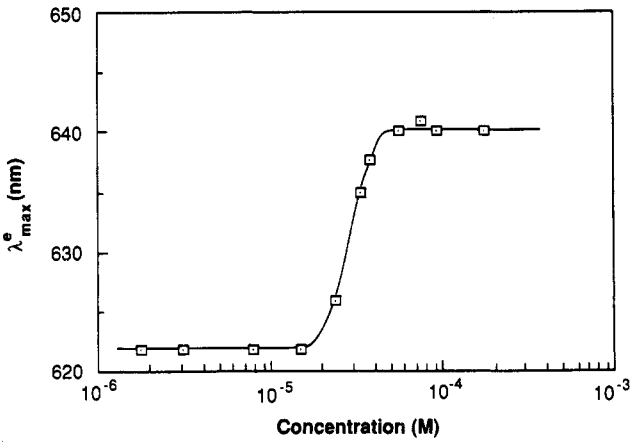

Figure 14. Concentration dependence of the emission maximum (λ_{max}^e) in DHTAP solutions in concentrated H_2SO_4.

in Table II. In general, the emission properties, and especially λ_{max}^e, strongly depend on the concentration of the solution and the solvent. Fluorescence intensity generally increased with increasing concentration at a fixed excitation wavelength, as would be expected.

Figure 14 shows the concentration dependence of λ_{max}^e for solutions of DHTAP in concentrated H_2SO_4. At concentrations of $\sim 2.0 \times 10^{-5}$ M or less, λ_{max}^e has a value of 622 nm, whereas at $\sim 5.0 \times 10^{-5}$ M or more λ_{max}^e has a value of 640 nm. Thus, a sharp transition in the nature of the excited state occurs in the narrow concentration range $(2–5) \times 10^{-5}$ M. Very similar concentration-dependent emission properties of DHTAP solution were observed at different excitation wavelengths. The concentration effects on the solution emission properties of the DHTAP/MSA complex in methanol are very similar to those of the pristine DHTAP in sulfuric acid, as indicated in Table II. An even wider difference between the λ_{max}^e values at the low and high concentrations is observed compared to pristine DHTAP. However, emission maximum of the DHTAP/MSA complex in DMF is 580 ± 2 nm and is independent of concentration up to 1.65×10^{-4} M.

Concentration and solvent dependence of the emission properties of DHTAP and its methanesulfonate complex, and particularly λ_{max}^e, is the principal feature of the data that must be elucidated. We attribute the observed concentration dependence of the emission spectra to *aggregation phenomena* in solution at high concentrations.

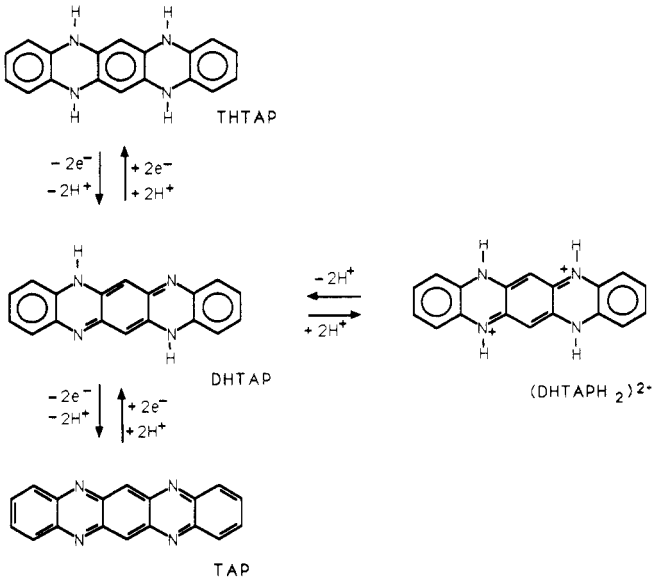

Figure 15. Some of the possible electron- and proton-transfer processes in DHTAP.

It is thus assumed that at sufficiently low concentrations the dicationic species of doubly protonated DHTAP (i.e., $DHTAPH_2^{2+}$) are fully ionized and dissociated, whereas at sufficiently high concentrations, dimeric or higher molecular weight aggregates of $DHTAPH_2^{2+}$ are formed. If such aggregates are formed in solution, it can be expected that due to the different effects of the aggregation and solvation on the excited states of the aggregated molecular system compared to the unaggregated molecular species, the observed results can be accounted for. Precedence for the effects of aggregation phenomena on the emission properties of organic molecules in solution exists,[29,35] for example, cationic polymethine cyanine dyes. An alternative explanation based on complex formation between DHTAP species and solvent molecules was ruled out, since similar concentration effects were observed in sulfuric acid where complex formation in solution exists and in methanol where $DHTAPH_2^{2+}(CH_3SO_3^-)_2$ is fully ionized in solution and is not expected to form a complex with MeOH.

Electrochemistry. There are many interesting aspects, as well as possible complications, in the electrochemistry of DHTAP and its derivatives because of the many possible electron- and proton-transfer processes, as shown in Figure 15. One question is the feasibility of electrochemical oxidation of the quinoidal DHTAP to the aromatic 5,7,12,14-tetraazapentacene (TAP). However, Badger and Pettit[30] have reported unsuccessful attempts to chemically oxidize DHTAP to TAP and, consequently, suggested that the quinoid system of DHTAP seems to be more stable than the aromatic system of TAP. These authors have also reported successful chemical reduction of DHTAP in solution to the colorless 5,7,12,14-tetrahydro-5,7,12,14-tetraazapentacene (THTAP), which rapidly oxidized in air back to DHTAP. One difficulty in trying to understand the redox properties of DHTAP is that it is only soluble in strong acids and the fact that the electrochemistry of imine (=N-) systems in acid solutions can be greatly complicated by accompanying protonation/deprotonation processes as is known in polyanilines[36,37] and benzimidazolebenzophenanthroline-type ladder polymer (BBL).[19,20] Badger and Pettit's results must be understood in this light, since their chemical redox reactions were performed in acid solutions. Our experiments and results on the electrochemistry of DHTAP and its derivatives are thus a preliminary study of a complicated electrochemical system.

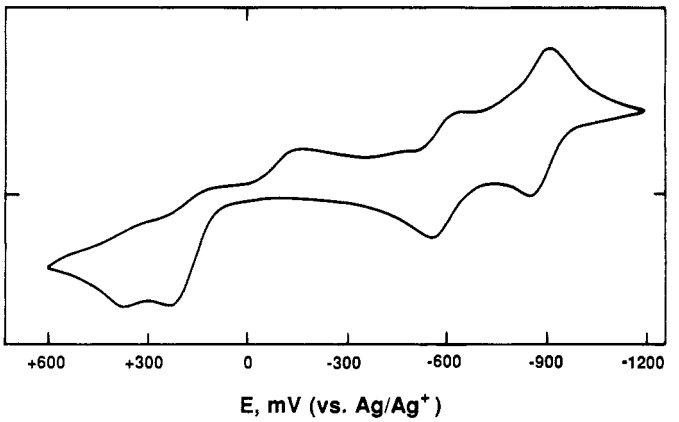

Figure 16. Cyclic voltammogram of 10^{-3} M DHTAP/MSA complex in DMSO/0.1 M TEAP at a 50 mV/s scanning rate.

Figure 16 shows a cyclic voltammogram (CV) of the DHTAP/MSA complex, i.e., $DHTAPH_2^{2+}(CH_3SO_3^-)_2$, in solution (0.1 M TEAP/DMSO). All the redox peaks are due to the complex, since a blank 0.1 M TEAP/DMSO showed no peaks in the potential range +600 to -1200 mV (vs Ag/Ag^+). The CV exhibits two reversible redox couples from which the first and second $E^{\circ\prime}$ values, each calculated as $(E_p^{ox} + E_p^{red})/2$, are obtained at -0.57 and -0.88 V (vs Ag/Ag^+). These $E^{\circ\prime}$ values are interpreted as the first and second reduction potentials of $DHTAPH_2^{2+}$ in solution. In addition, two irreversible oxidation peaks are observed at +0.23 and +0.37 V in the CV. These oxidation peak potentials cannot yet be assigned. Attempts to obtain a CV of pristine DHTAP in aqueous sulfuric acid solution were not successful; about four redox couples, all at potentials greater than 0 V (vs Ag/Ag^+), were always obtained but could not be reproduced.

Electrochemical behavior of polycrystalline thin films of unprotonated DHTAP on Pt flag (cast from dilute MSA or H_2SO_4 solutions) was also investigated by cyclic voltammetry at a scan rate of 100 mV/s. A large irreversible redox couple, with peak reduction and oxidation potentials at -955 and -626 mV (vs Ag/Ag^+), respectively, as well as electrochromism, was observed by cycling between +100 and -1900 mV. Both the redox couple and the electrochromism were stable to repeated cycling. The as-deposited thin film on the Pt electrode was gold-yellow in color, turning red (with patches of blue) after reduction at -955 mV and returning to gold-yellow upon oxidation at -626 mV. A detailed elucidation and delineation of the electron- and proton-transfer processes of DHTAP (see Figure 15) will require further studies of solution electrochemistry of DHTAP in conjunction with electronic absorption spectroscopy of the same species.

Electrical Conductivity. Compressed pellets of DHTAP had insulating electrical properties, the room-temperature dc conductivity being less than could be measured on our instruments ($\sigma_{RT} < 10^{-12}$ S/cm). Compressed pellets of DHTAP/MSA crystals had a σ_{RT} value of $\sim 4 \times 10^{-2}$ S/cm. Higher values of the conductivity were observed in a humid atmosphere, indicating moisture sensitivity of the samples. TGA studies showed that unbaked DHTAP/MSA complex can pick up up to 3–8% by weight moisture from the air. The conductivity also decreased on cooling to dry ice temperature, which suggests that the methanesulfonate salt of DHTAP is a semiconductor and not a metal. Even if the single-crystal room-temperature conductivity of the DHTAP/MSA salt is 2 orders of magnitude higher than the compressed pellet value of σ_{RT}, as is commonly observed, it is still quite small when compared to such charge-transfer salts[33,34] as *N*-meth-

ylphenazinium/TCNQ or TTF/TCNQ, which have single-crystal σ_{RT} values in the range of 100–1000 S/cm. The two possible primary factors that might explain the small conductivity value for the salt $(DHTAPH_2)^{2+}(CH_3SO_3^-)_2$ are as follows: (1) the complete charge transfer in the salt complex unlike partial or fractional charge transfer obtained in TTF/TCNQ and related salts; and (2) mixed stack crystals versus segregated stack crystals observed in TTF/TCNQ and related metallic salt complexes. However, it is not clear from our X-ray powder diffraction results if the crystal structure of the DHTAP/MSA complex is indeed of the mixed stack type.

Implications for High Molecular Weight Ladder Polyquinoxalines. The high molecular weight ladder polyhydroquinoxaline with a repeating unit molecular structure identical with DHTAP can be synthesized by a similar scheme except that the diamine is replaced by 1,2,4,5-tetraaminobenzene or its tetrahydrochloride.[9,38] Assuming a truly perfect ladder structure and a significantly higher degree of polymerization, the mechanical properties, melting, thermal stability, and solubility in solvents are obviously expected to be different from those of the model compound DHTAP. The electrochemistry of the high polymer is expected to be similar to the model compound. The optical properties, particularly the energy gap, are expected to improve with the degree of polymerization. Preliminary indications indeed show that the polymer (which is black in color) may have a much smaller band-gap.[38] It is not clear if *crystalline* salt complexes similar to DHTAP/MSA can be achieved in the polymer; however, similar complexation or redox reactions are expected to produce electrically conducting polymers. Overall, it is anticipated that the structural and physicochemical properties of the high molecular weight ladder polyquinoxalines would be similar enough to the model compound DHTAP that the present results would provide insights into the more complicated and less soluble high polymers.

Conclusions

The structural and physicochemical properties of a model compound of ladder polyquinoxalines, 5,12-dihydro-5,7,12,14-tetraazapentacene (DHTAP), have been investigated, including crystallization and melting, thermal stability, morphology, solubility, electronic absorption and emission, electrochemistry, complex formation, and electrical conductivity. DHTAP melts at 545 °C, close to its decomposition. The electronic absorption spectra of DHTAP in solution and in the solid state each exhibit two characteristic intense bands, near 300 and 600 nm, interpreted as π–π^* transitions.

DHTAP and its salt complexes exhibit strong fluorescence in solution, and the emission properties depend on concentration and solvent. The fluorescence emission maximum (λ_{max}^e) of DHTAP in concentrated H_2SO_4 in the concentration range of 10^{-6}–10^{-3} M, for example, exhibits a sharp transition from 622 to 640 nm at (2–5) × 10^{-5} M. The observed dependence of the fluorescence emission properties on concentration and solvent is attributed to aggregation phenomena in solution at the high concentrations.

It is shown that DHTAP forms a conductive crystalline complex with methanesulfonic acid (MSA) resulting in a methanesulfonate salt of the 7,14-protonated DHTAP: $(C_{18}H_{14}N_4)^{2+}(CH_3SO_3^-)_2$. Unlike the pristine unprotonated DHTAP, the DHTAP/MSA complex is soluble in many polar solvents and it has a room-temperature compressed pellet dc conductivity of about 10^{-2} S/cm. The highly anisotropic needlelike crystals of the DHTAP/MSA complex exhibit a melting point at 138 °C and decompose at about 300 °C.

The present results on the structural and physical properties of the model compound DHTAP and its complexes have direct implications for the high molecular weight ladder polyquinoxalines and will serve as a useful basis for comparison in subsequent studies of the related high polymers.

Acknowledgment. The technical assistance of James R. Peterson in synthetic and characterization efforts, Lee Hallgren in obtaining infrared and electronic absorption/emission spectra, and Dr. Robert Horning in obtaining the X-ray diffraction patterns is appreciated. This research was supported in part by the Air Force Wright Aeronautical Laboratories/Materials Laboratory under Contract No. F33615-85-C-5091 and performed while the author was at Honeywell, Inc., Physical Sciences Center.

References and Notes

(1) Van Deusen, R. L. *J. Polym. Sci., Polym. Lett.* **1966**, *B14*, 211–214.
(2) Arnold, F. E.; Van Deusen, R. L. *Macromolecules* **1969**, *2*, 497–503.
(3) Arnold, F. E.; Van Deusen, R. L. *J. Appl. Polym. Sci.* **1971**, *15*, 2035–2047.
(4) Arnold, F. E. *J. Polym. Sci., Part A-1* **1970**, *8*, 2079–2089.
(5) Bailey, W. J. In *Encyclopedia of Polymer Science and Technology*; Wiley: New York, Vol. 8, pp 97–120.
(6) Sicree, A. J.; Arnold, F. E.; Van Deusen, R. L. *J. Polym. Sci., Polym. Chem. Ed.* **1974**, *12*, 265–272.
(7) (a) Stille, J. K.; Mainen, E. *J. Polym. Sci., Polym. Lett. Ed.* **1966**, *4*, 39–41. (b) *Ibid.* **1966**, *4*, 665–667.
(8) Stille, J. K.; Freeburger, M. E. *J. Polym. Sci., Polym. Lett. Ed.* **1967**, *5*, 989–992.
(9) Stille, J. K.; Mainen, E. L. *Macromolecules* **1968**, *1*, 36–42.
(10) Imai, K.; Kurihara, M.; Mathias, L.; Wittman, J.; Alston, W. B.; Stille, J. K. *Macromolecules* **1973**, *6*, 158–162.
(11) Higgins, J.; Janovic, Z. *J. Polym. Sci., Polym. Lett. Ed.* **1972**, *10*, 301–303.
(12) Janovic, Z.; Higgins, J. *J. Polym. Sci., Part A-1* **1972**, *10*, 1609–1615.
(13) De Schryver, F.; Marvel, C. S. *J. Polym. Sci., Part A-1* **1967**, *5*, 545–552.
(14) Kellman, R.; Marvel, C. S. *J. Polym. Sci., Polym. Chem. Ed.* **1975**, *13*, 2125.
(15) Lee, B. H.; Marvel, C. S. *J. Polym. Sci., Polym. Chem. Ed.* **1983**, *21*, 83–87.
(16) Overberger, C. G.; Moore, J. A. *Adv. Polym. Sci.* **1970**, *7*, 113–150.
(17) (a) Ruan, J. Z.; Litt, M. H. *J. Polym. Sci., Polym. Chem. Ed.* **1987**, *25*, 285–297. (b) *Ibid.* **1987**, *25*, 299–309.
(18) (a) Kim, O. K. *J. Polym. Sci., Polym. Lett.* **1982**, *20*, 662. (b) Kim, O. K. *Mol. Cryst. Liq. Cryst.* **1984**, *105*, 161. (c) Kim, O. K. *J. Polym. Sci., Polym. Lett.* **1985**, *23*, 137–139.
(19) (a) Jenekhe, S. A.; Tibbetts, S. J. *J. Polym. Sci., Polym. Phys. Ed.* **1988**, *26*, 201–209. (b) Jenekhe, S. A.; Lo, S. K.; Flom, S. R., to be submitted for publication. (c) Jenekhe, S. A.; Vanherzeele, H., to be submitted for publication. (d) Jenekhe, S. A. *Extended Abstracts*, Electrochemical Society Meeting, Seattle, WA, Oct 14–19, 1990; Vol. 90-2, p 966.
(20) (a) Jenekhe, S. A. *Polym. Mater. Sci. Eng.* **1989**, *60*, 419–423. (b) Cao, X. F.; Jiang, J. P.; Block, D. P.; Hellwarth, R. W.; Yu, L. P.; Dalton, L. *J. Appl. Phys.* **1989**, *65*, 5012–5018. (c) Jenekhe, S. A.; Johnson, P. O. *Macromolecules* **1990**, *23*, 4419–4429.
(21) (a) Perkins, P. G. *Rev. Roum. Chim.* **1973**, *18*, 931–943. (b) *Ibid.* **1973**, *18*, 1111–1119.
(22) Wangbo, M. H.; Hoffmann, R.; Woodward, R. B. *Proc. R. Soc. London* **1979**, *A366*, 23–46.
(23) Kertesz, M.; Hoffmann, R. *Solid State Commun.* **1983**, *47*, 97–102.
(24) Bredas, J. L.; Themans, B.; Andre, J. M. *J. Chem. Phys.* **1983**, *78*, 6137–6148.
(25) Kivelson, S.; Chapman, O. *Phys. Rev. B.* **1983**, *28*, 7236–7243.
(26) (a) Yamabe, T.; Tanaka, K.; Ohzeki, K.; Yata, S. *Solid State Commun.* **1982**, *44*, 823–825. (b) Tanaka, K.; Ohzeki, K.; Nankai, S.; Yamabe, T.; Shirakawa, H. J. *Phys. Chem. Solids* **1983**, *44*, 1069–1075.

(27) (a) Robertson, J. M.; Sinclair, V. C.; Trotter, J. *Acta Crystallogr.* **1961**, *14*, 697–704. (b) Campbell, R. B.; Robertson, J. M.; Trotter, J. *Acta Crystallogr.* **1961**, *14*, 705–711. (c) Campbell, R. B.; Robertson, J. M.; Trotter, J. *Acta Crystallogr.* **1962**, *15*, 289–290.
(28) Silinsh, E. A. *Organic Molecular Crystals: Their Electronic States*; Springer-Verlag: New York, 1980.
(29) Simon, J.; Andre, J. J. *Molecular Semiconductors*; Springer-Verlag: Berlin and New York, 1985; pp 201 ff.
(30) Badger, G. M.; Pettit, R. *J. Chem. Soc.* **1951**, 3211–3215.
(31) (a) Wheland, R. C. *J. Am. Chem. Soc.* **1976**, *98*, 3926. (b) Wheland, R. C.; Gillson, J. L. *J. Am. Chem. Soc.* **1976**, *98*, 3916.
(32) Bryce, M. R.; Murphy, L. C. *Nature* **1984**, *309*, 119–126.
(33) Ferraris, J. P.; Cowan, D. O.; Walatka, V.; Perlstein, J. *J. Am. Chem. Soc.* **1973**, *95*, 948.
(34) Melby, L. R. *Can. J. Chem.* **1965**, *43*, 1448.
(35) (a) Jelley, E. E. *Nature* **1937**, *139*, 631. (b) Hofer, L. J. E.; Grabenstetter, R. J.; Wiig, E. O. *J. Am. Chem. Soc.* **1950**, *72*, 203. (c) Czikkely, V.; Forsterling, H. D.; Kuhn, H. *Chem. Phys. Lett.* **1970**, *6*, 11. (d) Daltrozzo, E.; Scheibe, G.; Gschwind, K.; Haimerl, F. *Photogr. Sci. Eng.* **1974**, *18*, 441. (e) Kopainsky, B.; Hallermeier, J. K.; Kaiser, W. *Chem. Phys. Lett.* **1982**, *7*, 87. (f) Mizutani, F.; Iijima, S.-I.; Tsuda, K. *Bull. Chem. Soc. Jpn.* **1982**, *55*, 1295.
(36) Michaelis, L.; Hill, E. S. *J. Am. Chem. Soc.* **1933**, *55*, 1488.
(37) (a) Diaz, A. F.; Logan, J. A. *J. Electroanal. Chem.* **1980**, *111*, 111. (b) Wnek, G. E. *Polym. Prepr. (Am. Chem. Soc., Div. Polym. Chem.)* **1986**, *27* (1), 277.
(38) Jenekhe, S. A.; Peterson, J. R., unpublished results.

Registry No. DHTAP, 531-47-5; DHTAP/MSA, 130469-35-1; *o*-phenylenediamine dihydrochloride, 615-28-1; 2,5-dihydroxy-*p*-benzoquinone, 615-94-1.